

The Halo Occupation Distribution of HI Galaxies

J. Stuart B. Wyithe¹, Michael J. I. Brown², Martin A. Zwaan³, Martin Meyer⁴

¹ *School of Physics, University of Melbourne, Parkville, Victoria, Australia*

² *School of Physics, Monash University, Clayton, Victoria 3800, Australia*

³ *European Southern Observatory, Karl-Schwarzschild-Str. 2, 85748 Garching b. München, Germany*

⁴ *School of Physics, University of Western Australia, Crawley, WA 6009, Australia*

Email: swyithe@unimelb.edu.au

30 October 2018

ABSTRACT

We perform an analysis of the spatial clustering properties of HI selected galaxies from the HI Parkes All Sky Survey (HIPASS) using the formalism of the halo occupation distribution (HOD). The resulting parameter constraints show that the fraction of satellite galaxies (i.e. galaxies which are not the central member of their host dark matter halo) among HIPASS galaxies is $< 20\%$, and that satellite galaxies are therefore less common in HIPASS than in optically selected galaxy redshift surveys. Moreover the lack of fingers-of-god in the redshift space correlation function of HIPASS galaxies may indicate that the HI rich satellites which do exist are found in group mass rather than cluster mass dark matter halos. We find a minimum halo mass for HIPASS galaxies at the peak of the redshift distribution of $M \sim 10^{11} M_{\odot}$, and show that less than 10% of baryons in HIPASS galaxies are in the form of HI. Quantitative constraints on HOD models from HIPASS galaxies are limited by uncertainties introduced through the small survey volume. However our results imply that future deeper surveys will allow the distribution of HI with environment to be studied in detail via clustering of HI galaxies.

Key words: cosmology: large scale structure, observations – galaxies: halos, statistics – radio lines: galaxies

1 INTRODUCTION

The cosmic star-formation rate has declined by more than an order of magnitude in the past 8 billion years (Lilly et al. 1996, Madau et al. 1996), a trend that is observed across all wavelengths (Hopkins 2004 and references therein). Why this decline has taken place, and what drives it are two of the most important unanswered questions in our current understanding of galaxy formation and evolution. One of the issues that will need to be addressed in order to answer this question is the role of environment. In cold dark matter cosmologies, gas cools and collapses to form stars within gravitationally bound *halos* of dark matter. These galaxies can then grow via continued star formation or via mergers with other galaxies. As galaxies of a given baryonic mass can only reside within dark matter halos above a particular dark matter mass, galaxies are biased tracers of the overall dark matter distribution.

In linear theory, the bias in the spatial clustering of dark matter halos relative to the underlying mass distribution is a function of halo mass but not of spatial scale. As a consequence, if the mass power-spectrum is known, the clustering of galaxies on large scales yields strong con-

straints on the masses of the dark matter halos in which they reside. On smaller scales, the simple relationship between galaxy clustering and halo mass breaks down. Firstly the mass power-spectrum is in the non-linear regime. More importantly, multiple galaxies can be distributed within individual halos (at separations $\lesssim 1$ Mpc), with the number of galaxies within halos of a given mass exhibiting some scatter. While this complicates the modelling of galaxy clustering, it enables measurements of spatial clustering of galaxies to determine how galaxies populate dark matter halos as a function of halo mass. Some understanding of these issues is provided by simulations and these can be (and have been) tested against observations of the spatial clustering of optically selected galaxies.

By understanding how galaxies populate dark matter halos, key insights may be obtained into how galaxies grow over cosmic time. For example, while the merger rate of dark matter halos is known, modelling the dynamical friction of sub-halos (and thus galaxies) in cosmological simulations is non-trivial and the rate of galaxy growth via merging has been uncertain as a consequence. Knowing how galaxies populate dark matter halos resolves this problem. In particular,

arXiv:0908.2854v1 [astro-ph.CO] 20 Aug 2009

consider a case where the timescale for dynamical friction following the merger of two dark matter halos is short compared with the Hubble time. In this case galaxies within these halos will also merge soon after, and satellite galaxies will be relatively rare. On the other hand, if the dynamical friction timescale is long, then the galaxies within these halos may remain as satellite galaxies for many Gyr. In this case satellite galaxies will be relatively common. Brown et al. (2008) show that the later scenario holds for the most massive dark matter halos, with much of the stellar mass in massive halos residing within satellite galaxies.

The way in which stellar mass populates dark matter halos has, to first order, been determined for optically selected galaxy samples. However little is known about how HI, the fuel for star-formation, populates group and cluster mass dark matter halos. HI galaxies in the Fornax region have been studied by Waugh et al. (2002), who found very few galaxies to be associated with the Fornax cluster. None of the HI detections in Waugh et al. (2002) are early-type galaxies. Moreover, only 2 of the HI detections have both Fornax redshifts and are within 1 degree (~ 300 kpc) of the cluster centre. These results may suggest that there is a central galaxy high mass cut-off near the Fornax cluster halo mass (which is $7 \times 10^{13} M_{\odot}$ according to Drinkwater et al. 2001). More recently Cortese et al. (2008) have used Arecibo to survey a 5 square degree region around Abell 1367. They find a uniform distribution of HI-selected galaxies throughout the volume (i.e. when observed in HI the Abell cluster 1367 disappears), and that HI deficiency does not vary significantly with cluster-centric distance. These authors also find no finger-of-god effect in the HI-selected galaxies (in a redshift-position diagram, rather than in a clustering analysis). Similarly, Verheijen et al. (2007) study Abell 963 and 2192 at $z = 0.2$ and find only one HI-selected galaxy within 1Mpc from the centre of each cluster. On the other hand, de Blok et al. (2002) find that there are HI galaxies in Sculptor and Centaurus with HI masses of $\sim 10^9 M_{\odot}$. However these clusters have dynamical masses ~ 1.5 orders of magnitude lower than that of the Fornax and Abel clusters discussed above, and the identification of these with the clusters is not definitive.

Thus there are many questions. For example, is HI stripped from galaxies entering cluster, group or lower mass halos? Is there a dark matter halo mass above which HI is heated or removed from galaxies? Is the HI content of galaxies largely a function of galaxy stellar mass or host dark matter halo mass? Do the stellar masses of HI selected galaxies grow largely via star-formation or galaxy mergers? These questions can be addressed using the observed clustering of HI selected galaxies to constrain models of how HI populates dark matter halos. A popular formalism for modeling clustering on small to large scales is termed the halo occupation distribution (HOD) model (e.g. Peacock & Smith 2000; Seljak 2000; Scoccimarro et al. 2001; Berlind & Weinberg 2002; Zheng 2004; Zehavi et al. 2004). The HOD model includes contributions to galaxy clustering from pairs of galaxies in distinct halos which describes the clustering in the large scale limit, and from pairs of galaxies within a single halo which describes clustering in the small scale limit. The latter contribution requires a parametrisation to relate the number and spatial distribution of galaxies within a dark matter halo of a particular mass. Measurements of the HOD

of optically selected galaxies provide some insights into how galaxies evolve. For example, in the most massive dark matter halos, central galaxy stellar mass is proportional to halo mass to the power of approximately $\sim 1/3$. Much of the stellar mass within these halos resides within satellite galaxies (e.g., Brown et al. 2008, Moster et al. 2009). This result implies that the mergers of dark matter halos do not always lead to mergers of galaxies, and as a consequence massive galaxy growth is slow relative to the rapid growth of dark matter halos. Whether this result is also true for lower mass star-forming galaxies is unknown at this time.

In recent years large galaxy redshift surveys such as SDSS and the 2dFGRS have enabled detailed studies of the clustering of in excess of 100000 optically selected galaxies in the nearby universe. By comparison, the largest survey of HI selected galaxies contains ~ 5000 sources, obtained as part of the HI Parkes All Sky Survey (HIPASS, Barnes et al. 2001), a blind HI survey of the southern sky. Meyer et al. (2007) have studied the clustering of these HI galaxies. Their analysis reached the conclusion of weak clustering of HI galaxies based on parametric estimates of correlation length (see also Basilakos et al. 2007), but did not study the clustering in terms of the host dark matter halo masses of the HIPASS sample. In this paper we revisit the clustering of HIPASS galaxies using the HOD model. There are systematic uncertainties in estimation of the observed clustering amplitude, arising from the selection function and small survey volume (Meyer et al. 2007), and our results show that this limits the precision with which conclusions from clustering can be made. Nevertheless we illustrate that the clustering of HIPASS galaxies already provides interesting constraints on the distribution of HI within the dark matter halo population.

This paper is organised as follows. We begin by summarising the clustering of HI galaxies in the HIPASS survey § 2. We then summarise the formalism for the real and redshift-space HOD models for the correlation function (§ 3), which is discussed relative to the HIPASS observations in § 4 and § 5 respectively. We discuss the satellite fraction in § 6 and summarise our findings in § 7. In our numerical examples, we adopt the standard set of cosmological parameters (Komatsu et al. 2008), with values of $\Omega_m = 0.24$, $\Omega_b = 0.04$ and $\Omega_Q = 0.76$ for the matter, baryon, and dark energy fractional density respectively, $h = 0.73$, for the dimensionless Hubble constant, and $\sigma_8 = 0.81$ for the variance of the linear density field within regions of radius $8h^{-1}$ Mpc.

2 CLUSTERING OF HIPASS GALAXIES

Meyer et al. (2007) computed the redshift space correlation function of HI selected galaxies from 4315 detections in the HIPASS catalogue (HICAT; Barnes et al. 2001; Meyer et al. 2004; Zwaan et al. 2004). Correlation functions were produced by weighting each galaxy pair equally (termed unweighted), and by weighting each pair in a way that corrects for the survey selection function and minimises the variance in the correlation function estimate (termed weighted). From the redshift space correlation function, Meyer et al. (2007) computed the real space correlation functions in both the weighted and unweighted cases, using in-

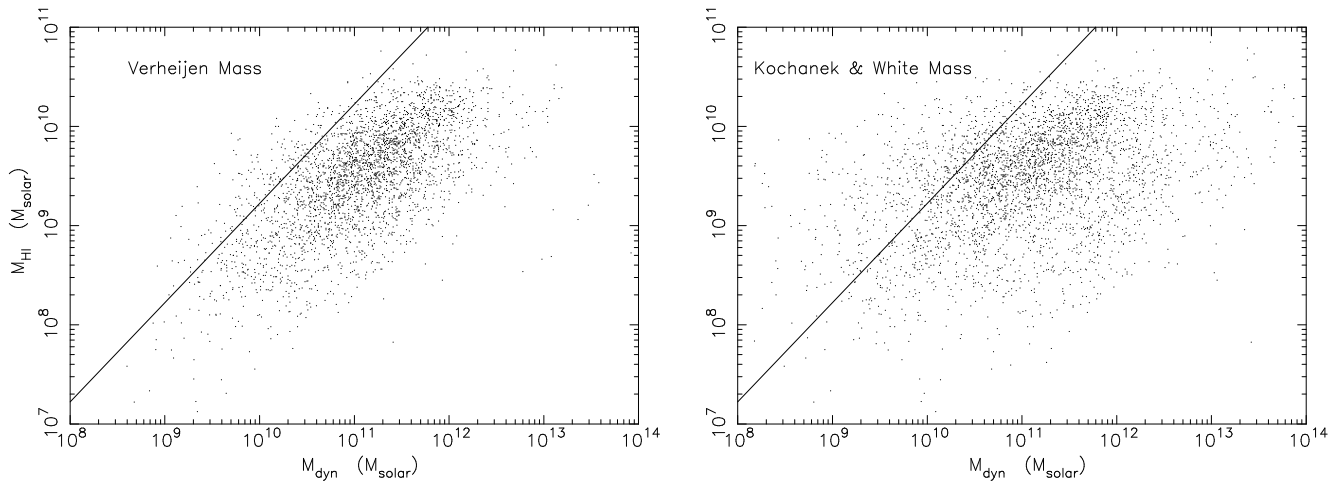


Figure 1. Plot of HI mass versus dynamical mass for HI galaxies in HIPASS. The left hand panel plots the HI mass against a dynamical mass estimated from the circular velocity using the methods of M. Verheijen, and by Kochanek & White (2001) respectively. The linear line shows the upper limit on HI mass of $M_{\text{HI}} \lesssim \Omega_{\text{b}}/\Omega_{\text{M}} M_{\text{dyn}}$.

versions that were both non-parametric and which assumed a powerlaw.

In this paper we restrict our attention to non-parametric estimates of the real space correlation function. However given the sensitivity of the measured clustering to the weighting scheme adopted, we fit both the unweighted and the weighted real-space correlation function from Meyer et al. (2007). From their estimated correlation function, Meyer et al. (2007) calculate a correlation length for the HIPASS galaxies. In this paper our aim is instead to interpret the astrophysical context of the measured clustering, namely the distribution of HI galaxies within the dark-matter halo population and the typical dark matter halo mass.

2.1 Density of HIPASS galaxies

Constraints on HOD models are provided both by the clustering of galaxies, and by the density of galaxies via comparison with the dark-matter halo mass function. We estimate the space density of HIPASS sources from the HI mass function (Zwaan et al. 2005a), yielding

$$n_{\text{gal}} = \theta_{\star} \Gamma(1 + \alpha, M_{\text{HI,lim}}/M_{\text{HI},\star}), \quad (1)$$

where $M_{\text{HI,lim}}$ is the lowest HI mass included in the calculation of space densities, and the parameters have measured values of $\alpha = -1.37$, $\theta_{\star} = 0.0060 \text{Mpc}^{-3}$, and $M_{\text{HI},\star} = 10^{9.8} M_{\odot}$. If all HIPASS galaxies with HI masses $> 10^7 M_{\odot}$ were included, the space density would be $n_{\text{gal}} \sim 0.15 \text{Mpc}^{-3}$. However HI masses of $10^7 M_{\odot}$ can only be detected out to very small distances in HIPASS, and so are not really represented in the calculation of the correlation function. A better estimate is obtained by looking at the peak of the redshift distribution, where the typical HI mass is $\sim 10^{9.25} M_{\odot}$. The space density for HI masses larger than $10^{9.25} M_{\odot}$ is $n_{\text{gal}} \sim 0.0069 \text{Mpc}^{-3}$. We estimate the error on this value to be $\sim 15\%$.

2.2 Dynamical masses of HIPASS galaxies

An analysis of the observed clustering of a galaxy population based on the bias of dark-matter halos implicitly assumes a relationship between galaxy luminosity (or in this case HI mass) and the host halo mass. Before proceeding to discuss the formalism for the model of halo clustering we therefore describe the relation between HI mass and dynamical mass for galaxies in the HIPASS survey. The dynamical mass M_{dyn} of the HI galaxies was estimated using the circular velocity (V_{c}) derived from the width of the HI spectrum using two methods. Firstly, based on the work of Marc Verheijen (PhD thesis), we have estimated the mass of a dark matter halo with a Hernquist (1990) profile using the relation $M_{\text{dyn}} = 10^{10} R (V_{\text{c}}/103.9 \text{km s}^{-1})^2 M_{\odot}$, where for the radius R , we have adopted the B-band Kron radius (measured in kpc). The resulting relation is shown in the left hand panel of Figure 1. Secondly, we have also estimated M_{dyn} from V_{c} based on Kochanek & White (2001), with results plotted in the right hand panel of Figure 1. Each panel includes a linear relationship to guide the eye, showing the upper limit on HI mass $M_{\text{HI}} \lesssim \Omega_{\text{b}}/\Omega_{\text{M}} M_{\text{dyn}}$. These panels illustrate that while there is significant scatter, larger HI masses are found in more massive host halos. Figure 1 illustrates that the relationship between HI and dynamical mass is shallower than linear, with $M_{\text{HI}} \propto M_{\text{dyn}}^{\gamma}$ where $\gamma \sim 0.5 - 0.7$. These dynamical masses are defined such that they are comparable to a definition based on the volume which encloses mass at ~ 200 times the mean density of the Universe.

The largest dynamical mass among the HIPASS sample is $\sim 10^{13} M_{\odot}$. For comparison, we expect a number $N \sim V_{\text{HIPASS}} \times M dn/dM = 300$ of halos in the HIPASS volume V_{HIPASS} , where we calculate dn/dM using the Sheth-Tormen (2002) mass function. This yields $N \sim 300$, 30 and 1 for masses of $M = 10^{13} M_{\odot}$, $10^{14} M_{\odot}$ and $10^{15} M_{\odot}$ respectively. Figure 1 shows that the observed number of these massive halos is much lower than the mass function predicts, although they should be detectable throughout the HIPASS search volume. Thus it appears that the most mas-

sive halos in the HIPASS volume do not host an HI galaxy which traces the halo potential.

3 HOD MODELS

In this paper we model the clustering of HIPASS galaxies using the halo occupation distribution formalism (HOD; e.g. Peacock & Smith 2000; Seljak 2000; Scoccimarro et al. 2001; Berlind & Weinberg 2002; Zheng 2004). Our approach is to fit HOD parameters for the non-parametric estimate of the real space HIPASS correlation function. Based on these fits, we then calculate the redshift-space correlation function using the analytic formalism described in Tinker (2007). In this section we describe the HOD modeling formalism briefly to provide context for the particular parametrisation used, and refer the reader to the above papers for details.

3.1 The real-space HOD model

The HOD model is constructed around the following simple assumptions. First, one assumes that there is either zero or one central galaxy that resides at the centre of each halo. Satellite galaxies are then assumed to follow the dark matter distribution within the halos. The mean number of satellites is typically assumed to follow a power-law function of halo mass, while the number of satellites within individual halos follows a Poisson (or some other) probability distribution.

The two-point correlation function can be decomposed into one-halo and two-halo terms

$$\xi(r) = [1 + \xi_{1h}(r)] + \xi_{2h}(r), \quad (2)$$

corresponding to the contributions to the correlation function from galaxy pairs which reside in the same halo and in two different halos respectively (Zheng 2004). In real space the 1-halo term can be computed using (Berlind & Weinberg 2002)

$$1 + \xi_{1h}(r) = \frac{1}{2\pi r^2 \bar{n}_g^2} \times \int_0^\infty dM \frac{dn}{dM} \frac{\langle N(N-1) \rangle_M}{2} \frac{1}{2R_{vir}(M)} F' \left(\frac{r}{2R_{vir}} \right). \quad (3)$$

Here \bar{n}_g is the mean number density of galaxies. We assume the Sheth-Tormen (1999) mass function dn/dM using parameters from Jenkins et al. (2001) throughout this paper. The distribution of multiple galaxies within a single halo is described by the function $F(x)$ which is the cumulative fraction of galaxy pairs closer than $x \equiv r/R_{vir}$. The contribution to F is divided into pairs of galaxies that do, and do not involve a central galaxy, and is computed assuming that galaxies follow the number-density distribution of a Navarro, Frenk & White (1997; NFW) profile (see e.g. Zheng 2004). The quantity $\langle N(N-1) \rangle_M$ is the average number of halo pairs. We assume an average distribution, with $\langle N(N-1) \rangle_M = \langle N \rangle_M^2 - \langle N \rangle_M$.

The 2-halo term can be computed as the halo correlation function weighted by the distribution and occupation number of galaxies within each halo. The 2-halo term of the galaxy power-spectrum is

$$P_{gg}^{2h}(k) = P_m(k) \left[\frac{1}{\bar{n}_g} \int_0^{M_{max}} dM \frac{dn}{dM} \langle N \rangle_M b_h(M) y_g(k, M) \right]^2, \quad (4)$$

where P_m is the mass power-spectrum and y_g is the normalised Fourier transform of the galaxy distribution profile (i.e. NFW). To compute the halo bias $b(M)$ we use the Sheth, Mo and Tormen (2001) fitting formula. The quantity M_{max} is taken to be the mass of a halo with separation $2r$. The 2-halo term for the correlation function follows from

$$\xi_{2h}(r) = \frac{1}{2\pi^2} \int_0^\infty P_{gg}^{2h}(k) k^2 \frac{\sin kr}{kr} dk. \quad (5)$$

On large scales the correlation function is sensitive only to the 2-halo term, and only to the number weighted galaxy bias. However on small scales, both the 1-halo and 2-halo terms contribute to the clustering, and the detailed shape of the correlation function is sensitive to the distribution of galaxies within halos. We use the following parametrisation to describe this distribution. Halos are assumed to host a single central galaxy and a number N_{sat} of satellite galaxies if their mass is in excess of M_{min} . The number of satellites is taken to be a powerlaw in mass with characteristic mass scale M_1 and index α . However, motivated by the fact that HI galaxies seem to be underrepresented as satellites in galaxy clusters (Waugh et al. 2002), we also include an upper limit for the halo mass which can contain an HI satellite ($M_{1,max}$). Thus the mean occupation of a halo of mass M is assumed to be

$$\begin{aligned} \langle N \rangle_M &= 1 + \langle M \rangle_{sat} & \text{if } M > M_{min} \\ &= 0 & \text{otherwise,} \end{aligned}$$

where the number of satellites is defined to be

$$\begin{aligned} \langle N \rangle_{sat} &= \left(\frac{M}{M_1} \right)^\alpha & \text{if } M_{min} < M < M_{1,max} \\ &= 0 & \text{otherwise.} \end{aligned}$$

3.2 The redshift space HOD model

Tinker (2007) has extended the above model to calculate the redshift space correlation function for a given HOD parametrisation. The redshift space model is again computed based on the sum of 1-halo and 2-halo terms as in equation (2). In redshift space, the apparent recession velocity of a galaxy is the sum of its motion in the Hubble flow (directly related to its physical distance), and of peculiar velocity (which modifies the apparent distance based on Hubbles constant). The 1-halo term is computed in analogy with equation (3), but with an additional integral over the line-of-sight distance and a probability distribution for the line of sight peculiar velocity. The result of these peculiar motions are the so-called fingers-of-god, large line-of-sight features in redshift. Tinker (2007) suggests that the 2-halo term of the redshift space correlation function at apparent line-of-sight (r_σ) and transverse (r_π) distances is most easily computed by integrating over the 2-halo term of the real space correlation function,

$$1 + \xi_{2h}(r_\sigma, r_\pi) = \int_{-\infty}^{\infty} [1 + \xi_{2h}(r)] P_{2h}(v_z|r, \phi) dv_z, \quad (6)$$

where $P_{2h}(v_z|r, \phi)$ is the probability density for the line-of-sight velocity between pairs in two distinct halos, and $\cos \phi = r_\sigma/r$. Here $z^2 = r^2 - r_\sigma^2$, and $v_z = H(r_\pi - z)$. Calculation of P_{2h} , including determination of fitting formulae to N-body simulations is complex and we refer the reader to Tinker (2007) for details.

4 REAL SPACE HOD MODELS OF HIPASS GALAXIES

In this section we describe fitting of HOD models to the real-space correlation function of HIPASS galaxies. Given the systematic uncertainty in the estimate of the correlation function owing to the small survey volume we follow Meyer et al. (2007) and choose to fit both the unweighted and weighted HIPASS correlation functions (although we note that the latter should more fairly estimate the correlation function that would be obtained from a larger, volume limited survey). Our HOD model has four free parameters, M_{\min} , M_1 , $M_{1,\max}$ and α , for combinations of which we compute the real space correlation function, and calculate the likelihood of the model as

$$\mathcal{L}(M_{\min}, M_1, M_{1,\max}, \alpha) = \exp(-\chi^2/2), \quad (7)$$

where

$$\chi^2 = \sum_{i=0}^{N_{\text{obs}}} \left(\frac{\log \xi(r_i | M_{\min}, M_1, M_{1,\max}, \alpha) - \log \xi_{\text{obs}}(r_i)}{\sigma_{\text{obs}}(r_i)} \right)^2 + \left(\frac{\log \bar{n}_{\text{g}}(M_{\min}, M_1, M_{1,\max}, \alpha) - \log n_{\text{gal}}}{\sigma_{\text{gal}}} \right)^2. \quad (8)$$

Here ξ_{obs} is the observed correlation function measured at a number (N_{obs}) of radii r_i , with uncertainty $\sigma_{\text{obs}}(r_i)$ (in dex), and n_{gal} is the observed galaxy density with uncertainty σ_{gal} (in dex). We compute the halo density \bar{n}_{g} using the Sheth-Tormen (2002) mass function as part of the HOD model. The error bars on the observational estimates are not symmetric. Note that we assume the correlation function points at different radii to be independent (as should be the case for a small sample, with large Poisson dominated noise). Covariance between measurements of the correlation function at different radii can lead to unrealistically small errors on constrained HOD model parameters. We do not add this layer of sophistication to our analysis, owing to the large uncertainties already introduced into the clustering measurements via the chosen weighting scheme.

We begin by fitting our HOD model to the unweighted real-space clustering of HIPASS galaxies. The upper row of the upper set of panels in Figure 2 shows contours of the likelihood in 2-d projections of this 4-d parameter space. Here prior probabilities on α , $\log M_{\min}$, $\log M_1$ and $\log M_{1,\max}$ are assumed to be constant. The contours are placed at 60%, 30% and 10% of the peak likelihood (the location of which is marked by a dot). The lower row shows the corresponding marginalised likelihoods on individual parameters. Meyer et al. (2007) noted that the correlation length of HIPASS galaxies is smaller than for optical surveys. Here we quantify the clustering on large scales via the host halo mass, finding a value of $M_{\min} \sim 10^{11.2 \pm 0.2} M_{\odot}$. On smaller scales, the halo occupation modeling illustrates the requirement of a non-zero 1-halo term in order to reproduce the excess clustering of galaxies at $r \lesssim 1$ Mpc. We find $M_1 \sim 10^{13.6 \pm 0.5} M_{\odot}$, which is two orders of magnitude larger than M_{\min} . The power-law index is tightly correlated with M_1 , but loosely constrained to be $\alpha \gtrsim 1$. Since M_1 represents the characteristic mass where satellites outnumber the central galaxies, the large value of M_1 indicates that there are only a small number of satellite galaxies in the HIPASS sample.

In the lower set of panels in Figure 2 we repeat this analysis for the weighted estimate of the HIPASS real-

space correlation function. Here we find best fit estimates of $M_{\min} \sim 10^{11.5 \pm 0.3} M_{\odot}$, and $M_1 \sim 10^{12.2 \pm 0.5} M_{\odot}$. There is greater tension between the galaxy density and clustering amplitude in this case leading to larger values of χ^2 for the best fit. We find $M_1 \sim 10 M_{\min}$, smaller than the difference found in the unweighted case. However the value of the power-law slope is loosely constrained to be $\alpha \sim 0.7 \pm 0.4$, weakly preferring satellites to be in smaller halos (but consistent with a linear relation). In this case M_1 and α are again tightly correlated, with a smaller value of M_1 associated with a shallower index α in order to produce the low amplitude of the small scale clustering.

If α is forced to equal unity in our analysis, then we find $M_1 = 10^{13} M_{\odot} \sim 50 - 100 M_{\min}$ for both the unweighted and weighted estimates. For comparison, with $\alpha = 1$, the red galaxy sample (chosen to exclude gas rich galaxies with a large star formation rate) from Brown et al. (2008) has clustering described by $M_1 \sim 3 M_{\min}$, while clustering of galaxies in the Sloan Digital Sky Survey (including both gas-rich and gas-poor galaxies) suggests $M_1 \sim 20 M_{\min}$ (Zehavi et al. 2005). Thus the qualitative conclusions of both the weighted and unweighted estimates of the HIPASS correlation function are consistent; namely that HI satellites in groups and clusters are rare compared to the results of optical clustering studies. We return to quantify this point further in § 6. The effect of satellites on the real space correlation function at small scales is illustrated in Figure 5 of Meyer et al. (2007), where it can be seen that HI selected HIPASS galaxies have a smaller correlation length than optically selected samples, but also that the difference in amplitude of the correlation function is greatest at scales less than 1 Mpc, where the 1-halo term dominates. Thus, by determining the relationship between M_{\min} and M_1 , the real space HOD correlation function quantifies previous suggestions that HI galaxies are under-represented in overdense environments (Waugh et al. 2002).

The inferred values of M_{\min} for the HIPASS galaxies are quantitatively consistent between the unweighted and weighted clustering estimates, making estimates of the halo mass for HIPASS galaxies fairly robust (we note that the estimates partly driven by the galaxy density, which is common between the two cases). Moreover, the clustering estimate of host mass from the unweighted HIPASS correlation function is easily reconciled with the dynamical estimates of HIPASS galaxy host masses shown in Figure 1, for which the logarithmic means are $\langle \log_{10}(M/M_{\odot}) \rangle = 11.1$ for both of the dynamical mass estimates presented.

4.1 The HI mass fraction in HIPASS galaxies

The halo mass estimates derived from the combination of clustering and density of HI galaxies allow the fraction of baryonic mass in galaxies that is in the form of HI (f_{HI}) to be estimated. To this end we first assume that the hydrogen to dark-matter mass ratio is the same within galaxies as in the mean universe, so that the total hydrogen mass within a halo of mass M is $\sim \Omega_{\text{b}}/\Omega_{\text{M}} M$. We then assume that the baryon to dark matter mass is the same for all halos, yielding

$$f_{\text{HI}} \sim \frac{\Omega_{\text{M}}}{\Omega_{\text{b}}} \frac{M_{\text{HI,lim}}}{M_{\min}}. \quad (9)$$

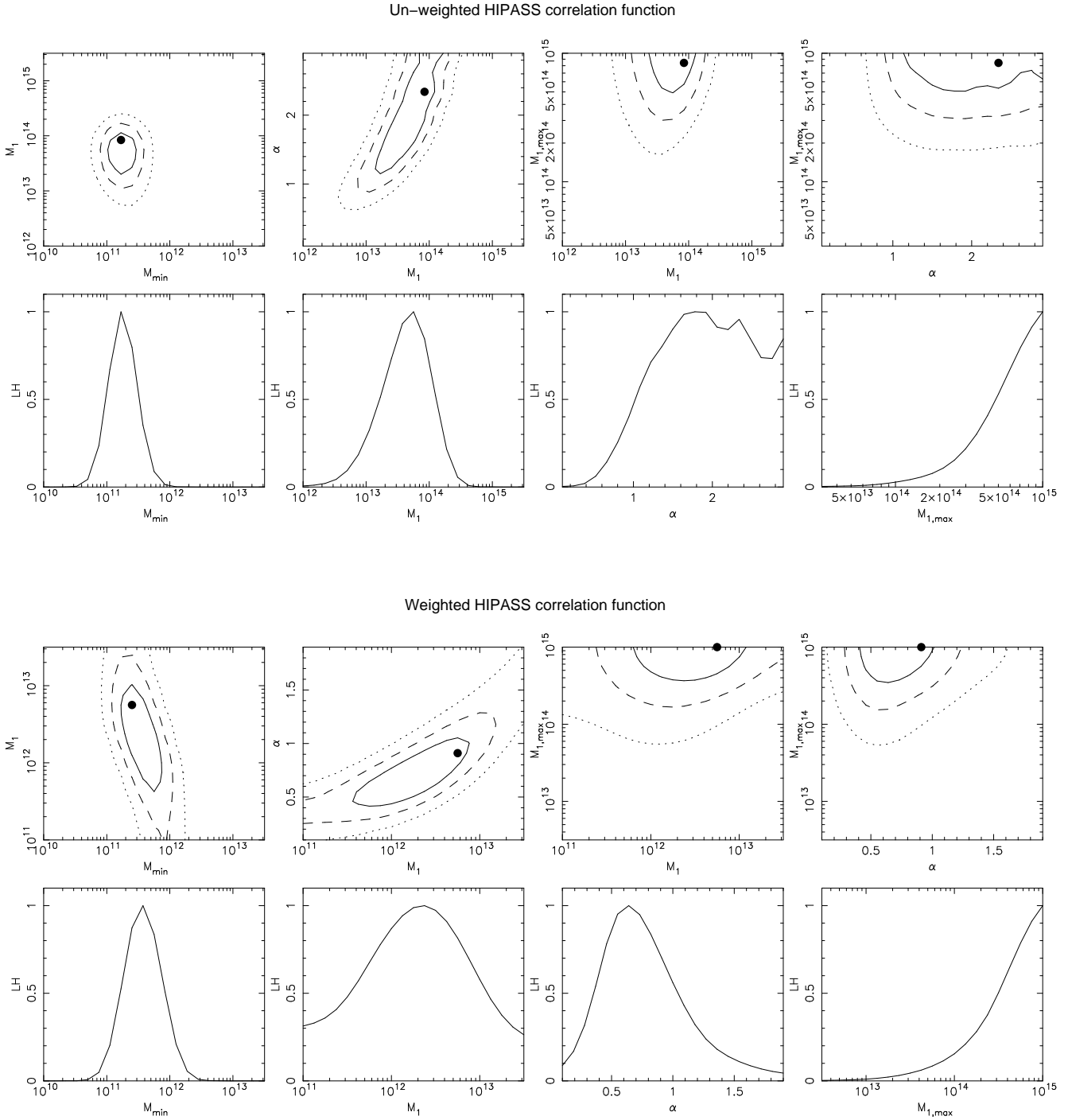


Figure 2. Constraints on HOD parameters describing estimates of the non-parametric real-space HIPASS correlation function from Meyer et al. (2007). Two sets of constraints are shown, based on the unweighted (upper set) and weighted (lower set) estimates of the HIPASS correlation function respectively. In each case, the *Upper panels* show contours of the likelihood in 2-d projections of the 4-d parameter space used for the HOD modeling, while the *Lower panels* show the marginalised likelihoods on individual parameters. Here prior probabilities on α , $\log M_{\min}$, $\log M_1$ and $\log M_{1,\max}$ are assumed to be constant. The contours are placed at 60%, 30% and 10% of the peak likelihood (the location of which is marked by a dot).

Un-weighted HIPASS correlation function

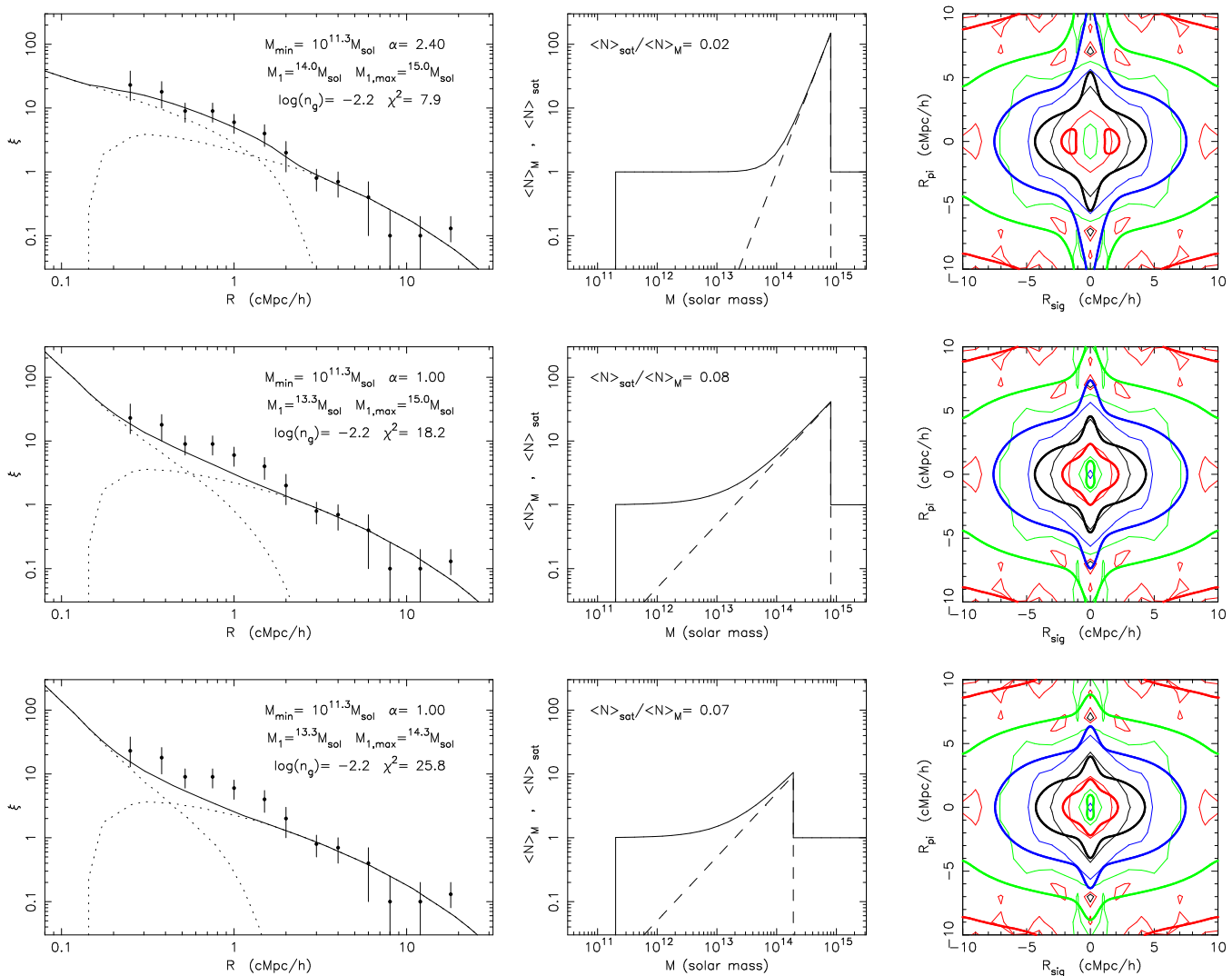


Figure 3. Examples of correlation functions that are consistent with the HOD parameter constraints in Figure 2 derived from the estimates of the unweighted real-space HIPASS correlation function. The *Left-hand panels* show modeled real-space correlation functions (with the 1-halo and 2-halo terms plotted as dotted curves). The non-parametric determinations of the real-space correlation function for HIPASS galaxies are plotted as the data points with error bars. The parameters used for each model are listed together with the resulting value of χ^2 . The *Central panels* show the corresponding total (solid lines) and satellite (dashed lines) occupation numbers of galaxies as a function of halo mass. The thick contours in the *Right-hand panels* show the corresponding redshift space correlation functions. The black contours correspond to $\xi = 1$, with the remaining contours differing in level by factors of 2. The model correlation function has been smoothed at $0.5h^{-1}\text{Mpc}$ for comparison with the data. The thin contours are the unweighted redshift-space correlation function for HIPASS galaxies (from Meyer et al. 2007).

Including the systematic uncertainty as estimated by the differing results for M_{\min} from the unweighted and weighted clustering measurements, we find $f_{\text{HI}} \sim 10^{-1.4 \pm 0.4}$. Thus we find that less than 10% of baryons within HI selected galaxies exists in the form of HI.

5 REDSHIFT SPACE HOD MODELS OF HIPASS GALAXIES

The line-of-sight structure of the redshift-space correlation function is dominated by gravitational infall on large transverse scales, and by virial motions of satellites on small

transverse scales. Both of these features can be seen in the unweighted HIPASS redshift space correlation function (plotted as the thin contours in the right hand panels of Figures 3 and 4), though the fingers-of-god are less pronounced than expected based on optical galaxy redshift surveys (Meyer et al. 2007). As mentioned above in § 2, the small volume of the HIPASS survey suggests that the correlation function should be constructed using a weighting scheme so that it is not dominated by galaxy pairs near the peak of the selection function. However this weighting introduces systematic uncertainty into the determination of the correlation function. The weighted redshift space correlation functions (plotted as the thin contours in the right

Weighted HIPASS correlation function

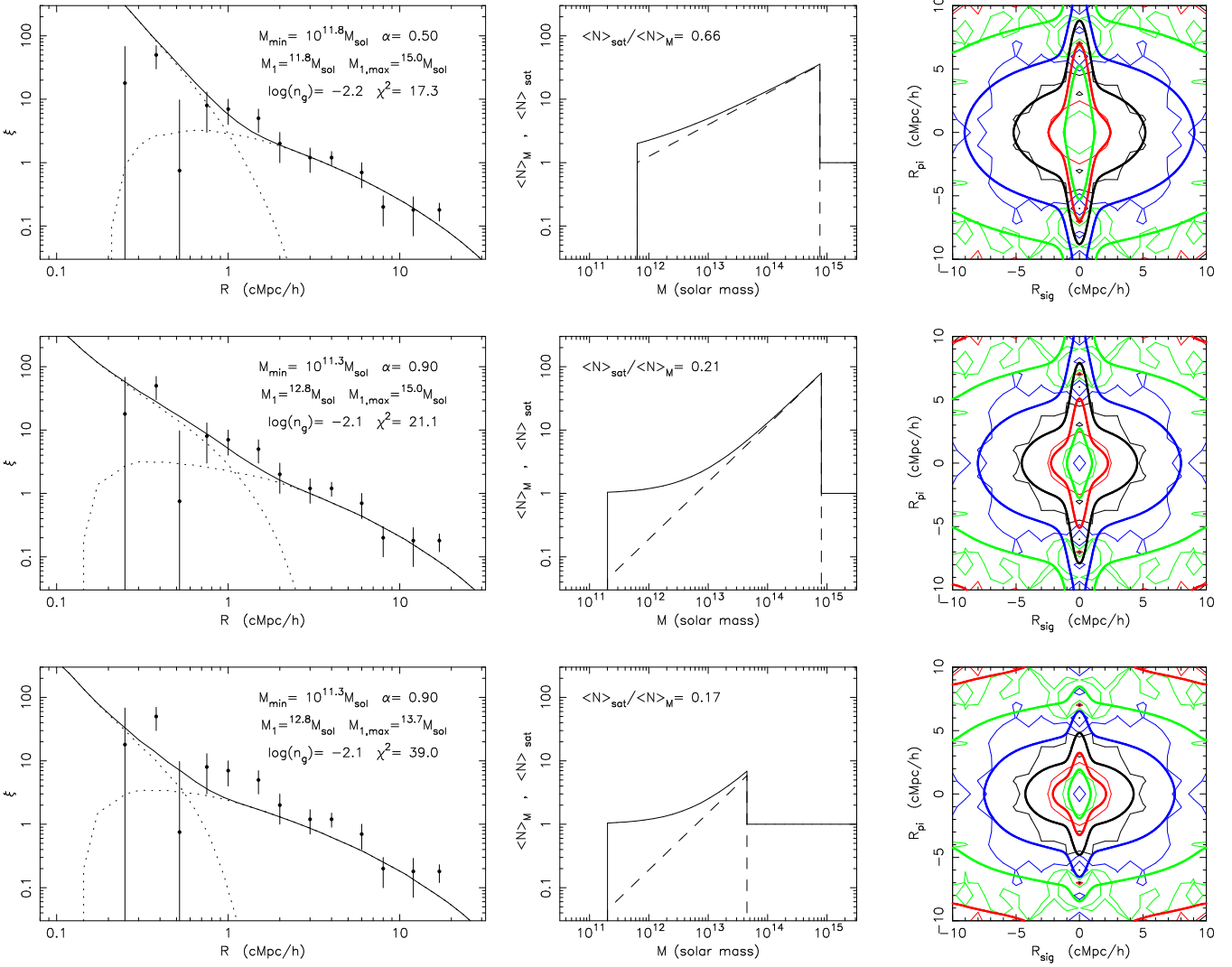


Figure 4. As per Figure 3, but showing examples of correlation functions that are consistent with the HOD parameter constraints in Figure 2 derived from the estimates of the weighted real-space HIPASS correlation function. The thin contours are the weighted redshift-space correlation function for HIPASS galaxies (from Meyer et al. 2007).

hand panel sets of Figure 4) show evidence for infall, but marginal or no evidence for fingers-of-god.

Additional information on the satellite galaxy distribution is contained in the redshift space correlation function. In redshift space, the line-of-sight structure of the 2-halo term is governed by gravitational infall, while the 1-halo term is dominated by the virial motions of satellite galaxies producing the so-called fingers-of-god. In this section we turn to calculation of the redshift space correlation function using the analytic HOD model of Tinker (2007). Given the large uncertainties in the construction of the HIPASS correlation function, we do not fit the redshift space correlation function directly. Rather, based on the parameter constraints in Figure 2 we calculate examples of the redshift space correlation function for qualitative comparison with the HIPASS clustering. These examples, and their comparison with the HIPASS redshift space correlation function, offer some hints regarding the satellite distribution that are

not available from the real space correlation function alone. They also indicate the way in which the full 3-dimensional shape of the correlation function could be utilized within a larger, more statistically representative sample.

Three examples are shown in each of Figures 3 and 4 for comparison with each of the unweighted and weighted determinations of the HIPASS correlation function. The chosen HOD models have parameters which adequately describe the real-space clustering, as shown in the left hand panels. In each case the models differ in the values chosen for various parameters. These values effect the occupation of dark matter halos as shown in the central panels of Figures 3 and 4. For example, smaller values of α and M_1 preferentially place the required number of satellites in smaller halos, and so reduce the prominence of the fingers-of-god. A smaller value of M_1 also lowers the typical mass at which satellites become common, and so increases the fraction of galaxies that are satellites (the fractions are listed in the central panels).

These two parameters are varied between the upper 2 panels of Figures 3 and 4). In the weighted case, the models also differ in the value of M_{\min} , with decreasing values from top to bottom. Larger values of M_{\min} (and hence larger values of bias) lead to smaller values of $\beta \equiv \Omega_m^{0.6}/b$, and in turn to a real-space correlation function that is less compressed along the line of sight on large transverse scales (as can be seen in the correlation functions of Figures 3 and 4). However the modeled fingers-of-god are more prominent than is the case in the HIPASS data for each of these cases.

In the lower panels of Figures 3 and 4 we show examples that impose an upper limit on the host mass containing satellite galaxies. By excluding the presence of satellites in massive halos, the values of $M_{1,\max} = 10^{14.3}M_\odot$ and $M_{1,\max} = 10^{13.7}M_\odot$ in the unweighted and weighted cases force the required number of satellites to reside in smaller halos. This reduces the prominence of the fingers-of-god, which are sensitive to the magnitude of satellite virial motions within the host halo. As a result these models yield fingers-of-god which are of comparable strength to those seen in the HIPASS data. On the other hand, these same fits to the unweighted estimate of the real-space correlation function predict line-of-sight compressions at large transverse separations [Kaiser (1987) effect] that appears to be too large to explain the HIPASS data¹. In the weighted case the correlation function amplitude is below the observed estimate owing to the tension between the density and correlation function amplitudes in this case.

6 SATELLITE FRACTION

Taken together the results of our modeling suggest that HI rich satellite galaxies are not common in HIPASS, or else the 1-halo term would be more prominent in the real-space correlation function. This is quantified in Figure 5, where we show the likelihoods (per unit logarithm) for the ratio $\langle N \rangle_{\text{sat}}/\langle N \rangle_M$ obtained by marginalising over the HOD distributions shown in Figures 3 and 4 for the unweighted and weighted HIPASS correlation functions respectively. A range of HOD models can describe the HIPASS real space correlation function, and our fits include a range of values with means near $\sim 3\%$ and $\sim 10\%$ for the fraction of satellites in the unweighted and weighted cases. Although unlikely, we find that the weighted estimate of the real space correlation function can be described with HOD models for which the satellite fraction is greater than 20%. However we find that HOD models which have more than 20% of the galaxies as satellites have fingers-of-god that are too prominent (e.g. see Figure 4). The satellite fraction of $\langle N \rangle_{\text{sat}}/\langle N \rangle_M \sim 0.20$ should therefore be considered an upper limit for HIPASS galaxies.

For comparison, typical fits to the halo occupation distribution of optical samples have satellite fractions that vary

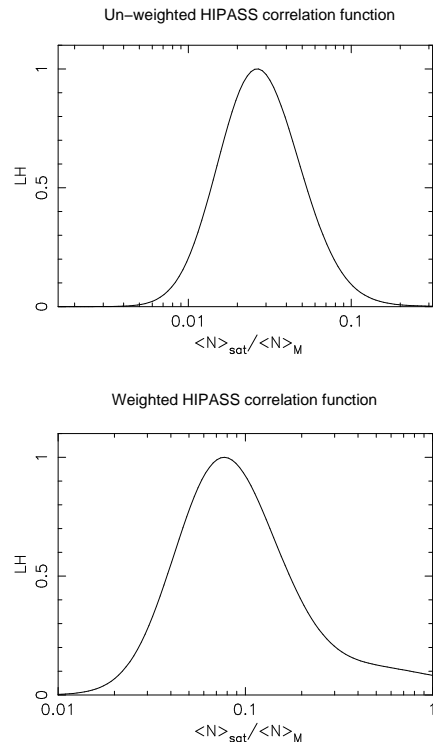


Figure 5. Likelihood functions (per unit logarithm) for the fraction of satellites among the HIPASS galaxies.

with galaxy luminosity and type. For example, the HOD modeling of Brown et al. (2008) implies a satellite galaxy fraction of $\langle N \rangle_{\text{sat}}/\langle N \rangle_M \sim 0.5$ among red galaxies with $0.2 < z < 0.4$ and a comparable space density to HIPASS. This suggests that red galaxies (which are HI poor) are more common among the satellite population than HI selected galaxies. On the other hand, for galaxies in the Sloan Digital Sky Survey with r-band absolute magnitudes in excess of -19 (again a sample with a comparable density to HIPASS galaxies) the HOD parametrization found in Zehavi et al. (2005) implies a satellite fraction of $\langle N \rangle_{\text{sat}}/\langle N \rangle_M \sim 0.25$. This value lies between the fraction we find from HIPASS, and the fraction found for red galaxies (Brown et al. 2008). Zehavi et al. (2005) divide their galaxy population into blue and red galaxies. They find that the red galaxy population has a steeper correlation function, which, when interpreted in terms of the HOD model implies that satellite galaxies are rarer among blue galaxies than among red galaxies. Thus there appears to be a sequence of satellite fractions. A sub-sample of red galaxies includes a larger proportion of satellites than does a sub-sample of blue galaxies, which in turn has a larger proportion of satellites than an HI selected sub-sample of galaxies.

Thus, as with observations of optical galaxy clustering, studying how HI galaxies populate dark matter halos provides important insights into how galaxies are assembled and evolve over cosmic time. For example, if massive galaxies grow largely via galaxy mergers rather than in-situ star formation, then star forming galaxies with large HI masses will be largely absent from the most massive dark matter halos. HI selected satellite galaxies will also be rare if HI galaxies merge rapidly after the merger of their host dark

¹ Note that we have plotted the redshift space correlation function using reflections of the measured correlation in the first quadrant to fill the remaining three quadrants. As a result, features due to noise in the correlation function are repeated and could give the impression of a systematic difference between the shape of the data and model correlation functions where no statistically significant difference exists.

matter halos. Similarly, if HI is consumed or removed from satellite galaxies within dark matter halos, then satellite galaxies would be under-represented in HI surveys relative to optical surveys as seems to be the case based on our analysis of HIPASS. Although our HOD results are suggestive of these scenarios, the precision with which the HI HOD can be studied with HIPASS is limited. However the much larger volumes that will become available with the advent of deeper HI surveys such as those to be undertaken with the Australian SKA Pathfinder (ASKAP, Johnston et al. 2008) will allow more detailed comparison of the halo occupation of stars and HI. This will in turn facilitate formulation of a more detailed understanding of the growth of stellar mass in galaxies.

7 SUMMARY

In this paper we have analysed the clustering properties of HI selected galaxies from the HIPASS survey using the formalism of the halo occupation distribution. Use of the HOD model separates the clustering amplitude into contributions from galaxy pairs that are in the same halo (the 1-halo term) and pairs that reside in different halos (the 2-halo term). The real-space clustering amplitude is significant on scales below the virial radius associated with the halo mass required to reproduce the clustering amplitude on large scales, indicating that single halo pairs are contributing a 1-halo term. However the resulting parameter constraints show that satellite galaxies make up only $\sim 10\%$ of the HIPASS sample. HI satellite galaxies are therefore less significant in number and in terms of their contribution to clustering statistics than are satellites in optically selected galaxy redshift surveys. Thus HOD modeling of HI galaxy clustering quantifies the extent to which environment governs the HI content of galaxies and confirms previous evidence that HI galaxies are relatively rare in overdense environments (Waugh et al. 2002; Cortes et al. 2008). Through our real-space modeling of HIPASS clustering we find a minimum halo mass for HIPASS galaxies at the peak of the redshift distribution of $M \sim 10^{11} M_{\odot}$, and show that less than 10% of baryons in HIPASS galaxies are in the form of HI.

Our analysis reveals significant degeneracies in the HOD parameters that give acceptable fits to the real-space HI correlation function. However the extra line-of-sight dimension in the redshift-space correlation function helps to break these degeneracies because the fingers-of-god are sensitive to the typical halo mass in which satellite galaxies reside. Our analysis of the redshift space correlation function indicates that in order to get fingers-of-god in a model which are as subtle as those in the HIPASS observations, the HI rich satellites required to produce the measured 1-halo term must be preferentially in group rather than cluster mass halos. In our modeling the best representations of the fingers-of-god are obtained by imposing an upper limit on the halo mass where HI satellites are found of $\sim 10^{13.7-14.3} M_{\odot}$. This finding is in accord with direct observations of rich optical clusters, which show no overdensity of HI galaxies relative to the field (Waugh et al. 2002; Cortes et al. 2008). Quantitative constraints on HOD models from the HIPASS survey are limited by the small survey volume, which makes the determination of the correlation function systematically un-

certain (Meyer et al. 2007). Future deeper HI surveys with telescopes like the Australian SKA Pathfinder (ASKAP) will survey a much larger volume (Johnston et al. 2008) and allow the distribution of HI with environment to be studied in more detail via precise measurements of clustering in HI galaxies.

The cosmic star-formation rate has declined by more than an order of magnitude in the past 8 billion years (Lilly et al. 1996, Madau et al. 1996). The decline is observed across all wavelengths (Hopkins 2004 and references therein) and apparently defies observational limitations such as sample selection and cosmic variance (Westra & Jones 2008). Optical studies paint a somewhat passive picture of galaxy formation, with the stellar mass density of galaxies gradually increasing and an increasing fraction of stellar mass ending up within red galaxies that have negligible star-formation (e.g., Brown et al. 2008). However optical studies can only address part of the picture. Currently, the combination of direct HI observations at low redshift (Zwaan et al. 2005b; Lah et al. 2007) and damped Ly α absorbers in the spectra of high-redshift QSOs (Prochaska et al. 2005) show that the neutral gas density has remained remarkably constant over the age of the universe. At these levels, and without replenishment, HI gas would be exhausted in a few billion years (Hopkins et al. 2008). Models incorporating gas infall that balances star formation and gas outflow are therefore necessary to reproduce observed star formation densities (eg. Erb 2008). The evolutionary and environmental relationships between the neutral gas which provides the fuel for star formation and the stars that form are central to understanding these and related issues. The study of the halo occupation distribution of HI based on HIPASS galaxies presented in this paper provides the first quantitative hints of this relationship.

Acknowledgments. The research was supported by the Australian Research Council (JSBW).

REFERENCES

- Barnes, D. G., et al. 2001, MNRAS, 322, 486
- Basilakos, S., Plionis, M., Kovač, K., & Voglis, N. 2007, MNRAS, 378, 301
- Berlind, A. A., & Weinberg, D. H. 2002, ApJ, 575, 587
- Brown, M. J. I., et al. 2008, ApJ, 682, 937
- Cortese, L., et al. 2008, MNRAS, 383, 1519
- de Blok, W. J. G., Zwaan, M. A., Dijkstra, M., Briggs, F. H., & Freeman, K. C. 2002, Astron. Astrophys., 382, 43
- Drinkwater, M. J., Gregg, M. D., & Colless, M. 2001, ApJL, 548, L139
- Erb, D. K. 2008, ApJ, 674, 151
- Hernquist, L. 1990, ApJ, 356, 359
- Hopkins, A. M. 2004, ApJ, 615, 209
- Hopkins, A. M., McClure-Griffiths, N. M., & Gaensler, B. M. 2008, ApJL, 682, L13
- Jenkins, A., Frenk, C. S., White, S. D. M., Colberg, J. M., Cole, S., Evrard, A. E., Couchman, H. M. P., & Yoshida, N. 2001, MNRAS, 321, 372
- Johnston, S., et al. 2008, Experimental Astronomy, 22, 151
- Kaiser, N., 1987, Mon. Not. R. Astron. Soc, 227, 1
- Kochanek, C. S., & White, M. 2001, ApJ, 559, 531

- Komatsu, E., et al. 2008, ArXiv e-prints, 803, arXiv:0803.0547
- Lah, P., et al. 2007, MNRAS, 376, 1357
- Lilly, S. J., Le Fevre, O., Hammer, F., & Crampton, D. 1996, ApJL, 460, L1
- Madau, P., Ferguson, H. C., Dickinson, M. E., Giavalisco, M., Steidel, C. C., & Fruchter, A. 1996, MNRAS, 283, 1388
- Meyer, M. J., et al. 2004, MNRAS, 350, 1195
- Meyer, M. J., Zwaan, M. A., Webster, R. L., Brown, M. J. I., & Staveley-Smith, L. 2007, ApJ, 654, 702
- Moster, B. P., Somerville, R. S., Maulbetsch, C., van den Bosch, F. C., Maccio', A. V., Naab, T., & Oser, L. 2009, arXiv:0903.4682
- Navarro, J. F., Frenk, C. S., & White, S. D. M. 1997, ApJ, 490, 493
- Peacock, J. A., & Smith, R. E. 2000, MNRAS, 318, 1144
- Prochaska, J. X., Herbert-Fort, S., & Wolfe, A. M. 2005, ApJ, 635, 123
- Scoccimarro, R., Sheth, R. K., Hui, L., & Jain, B. 2001, ApJ, 546, 20
- Seljak, U. 2000, MNRAS, 318, 203
- Sheth, R. K., & Tormen, G. 2002, MNRAS, 329, 61
- Sheth, R.K., Mo, H.J. & Tormen, G., 2001, Mon. Not. R. Astron. Soc., 323, 1
- Tinker, J. L. 2007, MNRAS, 374, 477
- Verheijen, M., van Gorkom, J., Szomoru, A., Dwarakanath, K. S., Poggianti, B., & Schiminovich, D. 2007, New Astronomy Review, 51, 90
- Waugh, M., et al. 2002, MNRAS, 337, 641
- Westra, E., & Jones, D. H. 2008, MNRAS, 383, 339
- Zehavi, I., et al. 2004, ApJ, 608, 16
- Zehavi, I., et al. 2005, ApJ, 630, 1
- Zheng, Z. 2004, ApJ, 610, 61
- Zwaan, M. A., et al. 2004, MNRAS, 350, 1210
- Zwaan, M. A., Meyer, M. J., Staveley-Smith, L., & Webster, R. L. 2005a, MNRAS, 359, L30
- Zwaan, M. A., van der Hulst, J. M., Briggs, F. H., Verheijen, M. A. W., & Ryan-Weber, E. V. 2005b, MNRAS, 364, 1467